Supplementary data

Lipid-Assisted PEG-*b*-PLA Nanoparticles with Ultrahigh SN38 Loading Capability for Efficient Cancer Therapy

Xiaoyi Huang, Jieyi Li, Yanfang Yang, Zi-Lu Wang, Xian-Zhu Yang, Zi-Dong Lu*, Cong-Fei Xu*

Experimental

***In vitro* drug release test**. SN38-loaded lipid-assisted PEG-*b*-PLA nanoparticles prepared using different charged lipids were tested for *in vitro* release of SN38 in triplicates in phosphate buffered saline (PBS, 10 mM, pH 7.4) containing 0.5% (w/v) SDS. Specifically, nanoparticles containing 0.2 mg SN38 were suspended in 1 mL PBS in a dialysis tubing (Spectra Por 1 membrane, 12 kDa cut-off). This dialysis tubing was placed in a screw-capped tube containing 40 mL PBS supplemented with 0.5% (w/v) SDS. The tubes were shaken at 200 rpm on a horizontal water bath shaker maintained at 37 ± 0.5ºC. At predetermined time intervals, the whole medium in the tube was withdrawn and replaced by fresh PBS supplemented with SDS to maintain sink conditions. The aliquots were assayed for the concentration of SN38 released by HPLC analysis as mentioned before.

Molecular dynamics (MD) simulation. A total of three simulation systems, including the pure SN38 system, the SN38/DOTAP system and the SN38/PEG-*b*-PLA system were constructed. MD simulation was carried out under constant temperature, constant pressure and periodic boundary conditions using Gromacs 2018.4 program. GAFF all-atomic force fields were applied for all the molecular force field.[1] In the MD simulation process, LINCS algorithm was used to constrain all hydrogen bonds,[2] and the integral step was 2 fs. The electrostatic interaction is calculated using the Particle-

mesh Ewald (PME) method.[3] The non-bond interaction cutoff value is set to 10 Å and updated every 10 steps. The simulated temperature was controlled at 298.15 K by V-rescale temperature coupling method,[4] and the pressure was controlled at 1 bar by Parrinello-Rahman method.[5] Firstly, the steepest descent method is used to minimize the energy of the three systems to eliminate the too close contact between atoms. Then, 100 ps NVT balance simulation was performed at 298.15 K. Finally, MD simulation of 100 ns was performed on three different systems respectively, and conformation was saved every 10 ps. Visualization of simulation results was completed by Gromacs embedded program and VMD.

Hemolysis analysis. Hemolysis assays were carried out according to the method reported by Nadhman et al. with some modification.[6] Rabbit erythrocytes were used for the testing since their hemolytic characteristics are the closest to that of human. Specifically, 10 mL of rabbit blood was collected from arteria cruralis of New Zealand albino rabbits into heparinized vacutainers and the fibrinogen was removed by stirring with a glass rod. The defibrinogen blood sample was centrifuged at 3000 rpm for 10 min and the erythrocyte pellets were washed four times with 0.9% saline. Finally, the erythrocyte pellets were resuspended in 0.9% saline to give a 2% erythrocyte standard dispersion. SN38 loaded nanoparticles suspended in 0.9% saline solution were added to the erythrocyte suspensions with final concentration between 0.4 and 10 μg/mL of SN38 and incubated at 37 °C for 3 h. Positive control was prepared by adding an equal volume of ddH2O into 2% erythrocyte standard dispersion instead of 0.9% saline and SN38 loaded nanoparticle suspensions. The tubes were centrifuged for 10 min at 3000 rpm, and the absorbance of the supernatant was measured at 576 nm. The percentage of hemolysis was calculated according to the equation below. Each treatment was done in triplicates.

$$\text{Hemolysis (\%)} : \frac{\text{Abs of sample - Abs of negative control}}{\text{Abs of positive control - Abs of negative control}} \times 100$$

Cell lines and animals. The human colorectal cancer cell lines (HCT 116 and HT-29) and human pancreatic cancer cell line (BxPC-3) were all obtained from the

American Type Culture Collection (ATCC). HCT 116 and HT-29 cells were cultured in McCoy's 5A medium (containing 10% FBS) in a humidified atmosphere containing 5% CO_2 at 37 °C, and BxPC-3, MCF-7, A549, and SKOV3 cells were cultured in 1640 medium (containing 10% FBS). BALB/c female nude mice (4–5 weeks' old), ICR female mice (6 weeks' old) and KM female mice (6 weeks' old) were purchased from the Beijing Vital River Laboratory Animal Technology Co., Ltd. (Beijing, China) and all animals received care in accordance with the guidelines set out in the Guidelines for the Care and Use of Laboratory Animals. Operation was approved by the South China University of Technology Animal Care and Use Committee. To establish the xenograft colorectal tumor or pancreatic carcinoma model, 50 μL of HCT 116 or HT-29 or BxPC-3 (1×10^6 cells) diluted in 20% matrigel (BD Bioscience, Franklin Lakes, NJ) were subcutaneously injected into the right flank of the BALB/c nude mice. The animals were randomly assigned to groups (n = 5–6) when the tumor sizes approached about 50–150 mm^3.

Cellular uptake by flow cytometry analysis. HCT 116 cells were plated in 24-well plate at 5×10^4 cells per well. SN38-loaded nanoparticles diluted to specific concentrations of SN38 (10 μg/mL) by McCoy's 5A medium was added into the HCT 116 cells. After 4−8 hours' incubation, cells were harvested and washed with PBS three times and trypsinized into single cells. Finally, the cells were subjected to flow cytometry (FACS) analysis on a BD Accuri C6 plus (BD Biosciences, USA).

Blood biochemical assay. BALB/c nude mice or KM mice were *i.v.* injected with Saline, CPT-11 and SN38 loaded nanoparticles at an equivalent dose of 15 mg kg^{-1} (for antitumor efficacy study) or 25−55 mg kg^{-1} (for single dose acute toxicity study) SN38. The blood was collected without adding anticoagulant on specified days after treatment or at the end of the treatment for biochemical analysis using a 3100-type automatic biochemical analyzer (Hitachi Co., Tokyo, Japan).

Statistical analysis. All results are expressed as mean ± SD. Statistical analysis was analyzed using an unpaired Student's *t*-test (two-tailed) for two groups, and one-way ANOVA with Tukey's multiple comparisons. Significance levels were defined as

ns: no significant difference, $P > 0.05$, *$P < 0.05$, **$P < 0.01$, and ***$P < 0.001$, P values were calculated by GraphPad Prism v8.3.0 (GraphPad Software, San Diego, CA).

References

1. W.L. Jorgensen, J. Chandrasekhar and J.D. Madura, *J. Chem. Phys.*, 1983, **79**, 926−935.

2. B. Hess, H. Bekker, H.J.C. Berendsen and G.E.M.J. Fraaij, *J. Chem. Theory Comput.*, 1997, **4**, 1463−1472.

3. T.A. Darden,; D.M. York and L.G. Pedersen, *J. Chem. Phys.*, 1992, **98**, 10089−10092.

4. H.J.C. Berendsen,; J.P.M. Postma, W.F. Van Gunsteren, A. DiNola and J.R. Haak, *J. Chem. Phys.*, 1984, **81**, 3684−3690.

5. R. Martonák, A. Laio and M. Parrinello, *Phys. Rev. Lett.*, 2003, **90**, 075503.

6. A. Nadhman, S. Nazir, M.I. Khan, A. Ayub, B. Muhammad, M. Khan, D.F. Shams and M. Yasinzai, *Int. J. Nanomed.*, 2015, **10**, 6891−6903.
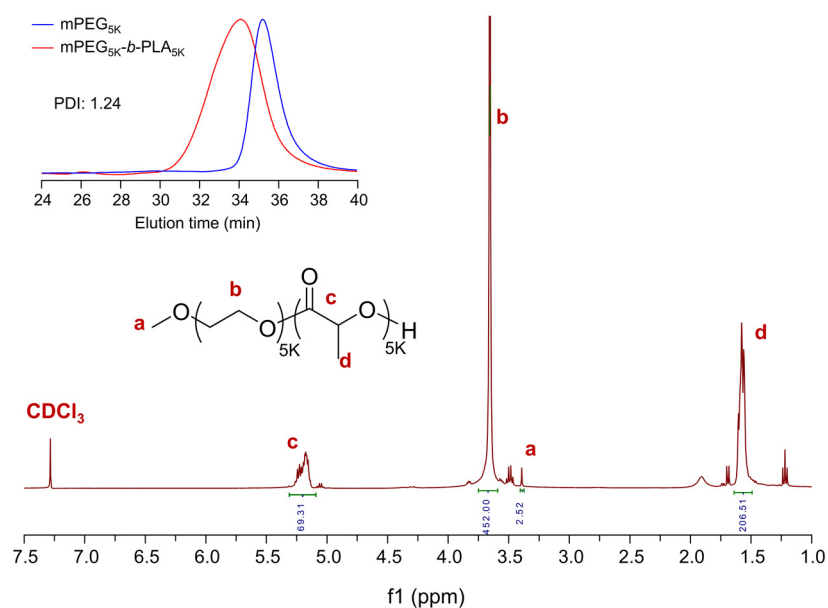
Fig. S1 Structure and molecular weight of PEG-*b*-PLA were verified by ^{1}H-nulcear magnetic resonance (^{1}HNMR) and gel permeation chromatography (GPC) (inserted

graph).
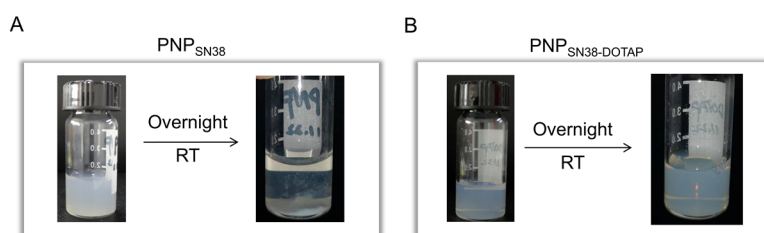
Fig. S2 Images of the appearance of different nanoparticle suspensions during storage at room temperature.
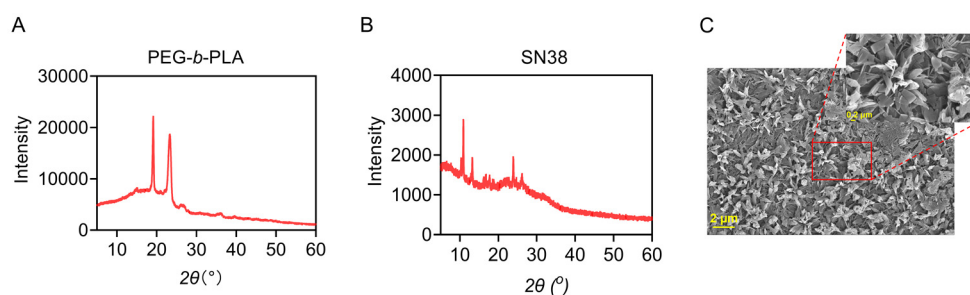

Fig. S3 (A-B) XRD analysis of PEG-*b*-PLA and SN38 respectively. (C) SEM analysis of SN38. Scale bar: 2 μm.
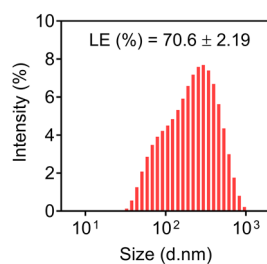

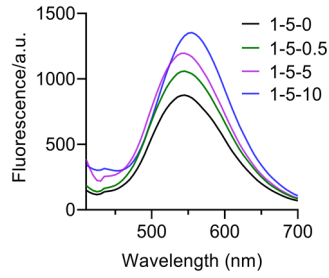**Fig. S4** DLS analysis of NP$_{SN38-DOTAP}$ without adding PEG-*b*-PLA. LE (%): loading efficiency (%).

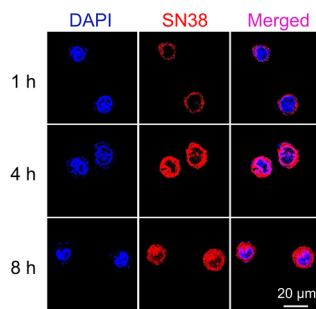**Fig. S5** Fluorescence emission spectra of different nanoparticle formulations at different weight ratios of SN38:PEG-*b*-PLA:DOTAP.

Fig. S6 CLSM analysis of cellular uptake profiles of PNP$_{SN38-DOTAP}$.
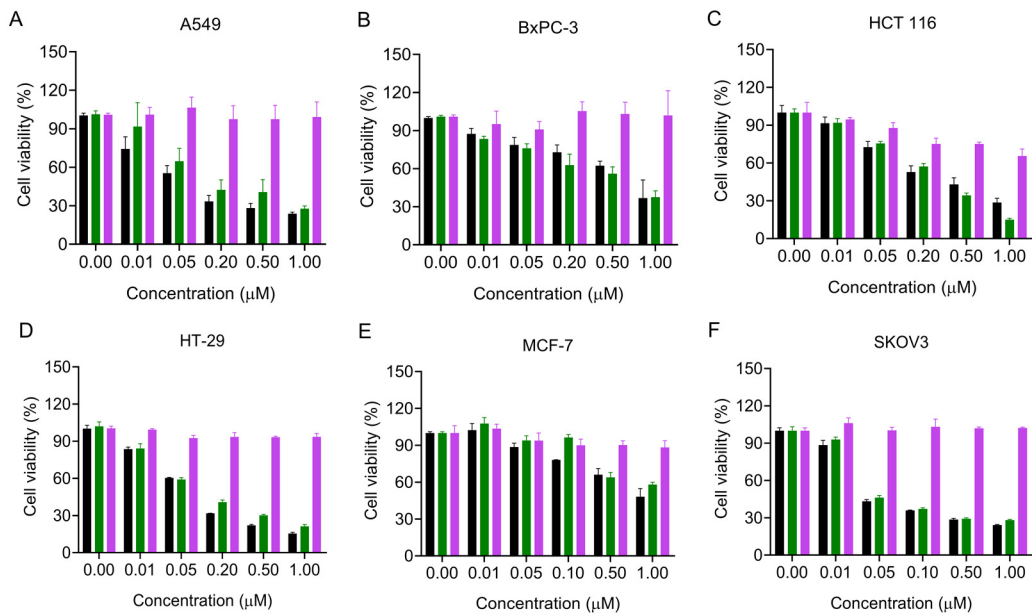
Fig. S7 Viabilities of various cell lines after incubation with different drug formulations by MTT assay. Black: free SN38; Green: PNP$_{SN38-DOTAP}$; Purple: CPT-11.
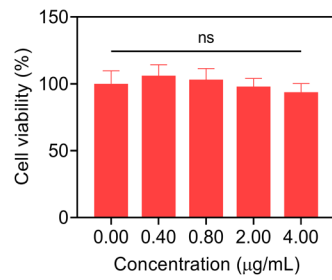
Fig. S8 Viabilities of HCT 116 cells after incubation with blank drug carrier prepared from PEG-*b*-PLA and DOTAP by MTT assay.
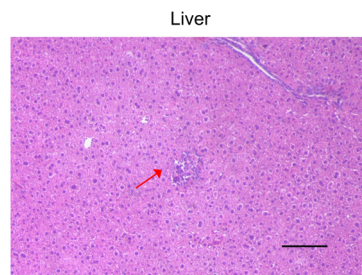

Fig. S9 Hematoxylin/eosin (H&E) assay of the liver from the CPT-11 group at the end of treatment. Scale bar: 100 μm. Damage to the tissues or cells was marked with red arrows.
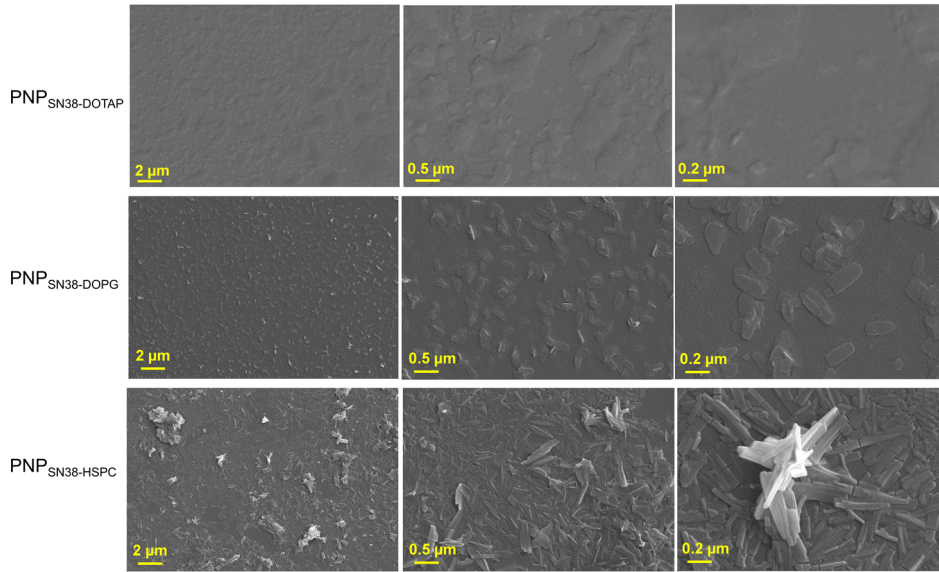
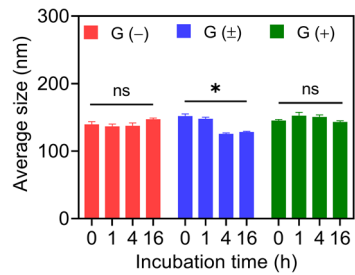**Fig. S10** SEM analysis of different films including PNP$_{\text{SN38-DOTAP}}$, PNP$_{\text{SN38-DOPG}}$, and PNP$_{\text{SN38-HSPC}}$.

Fig. S11 The size changes of PNP$_{\text{SN38-DOTAP}}$ (G(+)), PNP$_{\text{SN38-DOPG}}$ (G(−)), and PNP$_{\text{SN38-HSPC}}$ (G(±)) during incubation with cell culture medium (*i.e.* DMEM medium plus 10% FBS) at 37 °C.
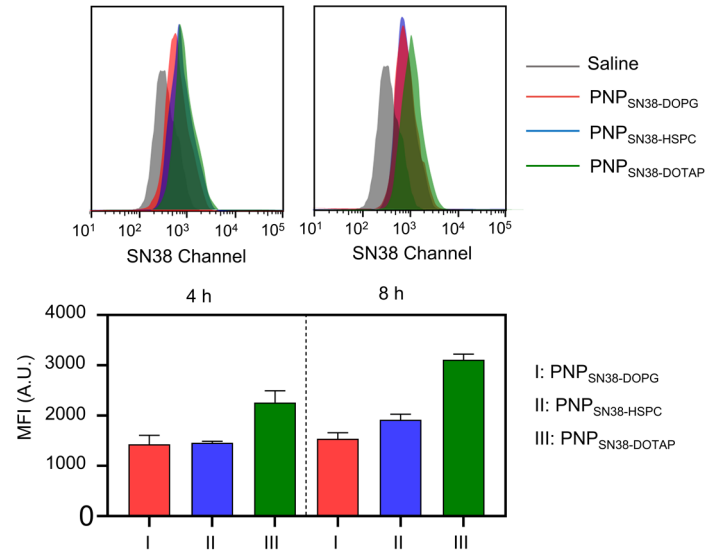
Fig. S12 Cellular uptake of cationic, anionic and neutral lipid-assisted PEG-*b*-PLA nanoparticles by HCT 116 cells using flow cytometry analysis.
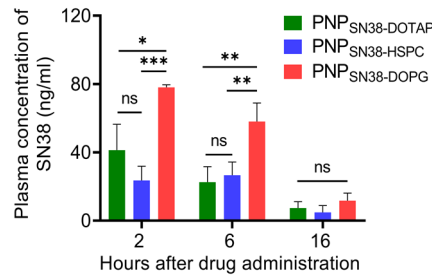

Fig. S13 *In vivo* plasma drug concentrations of SN38 after intravenous administration with cationic, anionic and neutral lipid-assisted PEG-*b*-PLA nanoparticles.
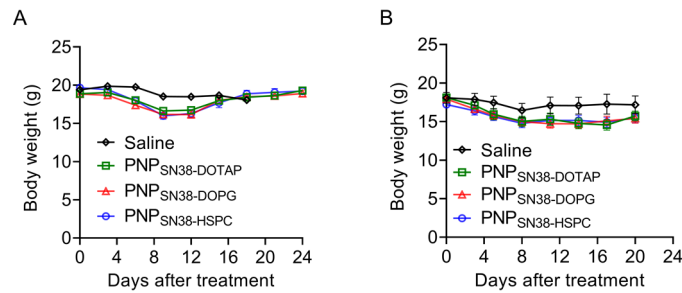

Fig. S14 Body weight change of mice after various treatments. (A) Xenograft HCT 116 colorectal tumor model. (B) Xenograft HT-29 colorectal tumor model.
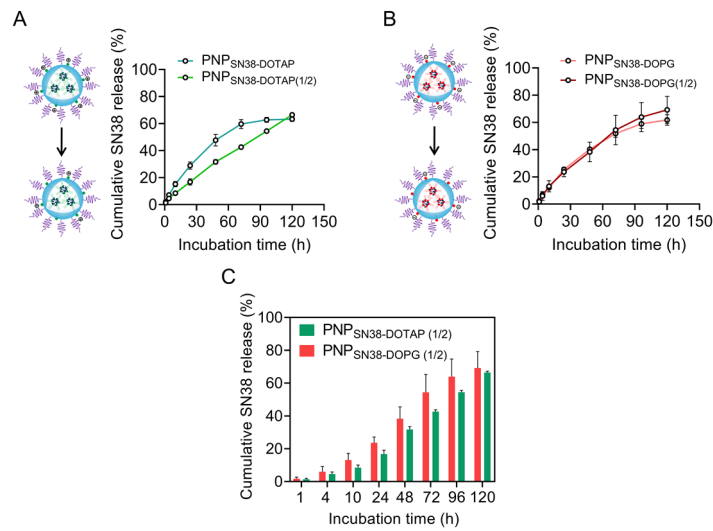
Fig. S15 *In vitro* drug release profiles of different charged SN38-loaded nanoparticles in PBS medium (10 mM, pH = 7.4). (A) The effect of DOTAP content on the drug release profile of SN38. (B) The effect of DOPG content on the drug release profile of SN38. (C) The effect of lipid type on the drug release profile of SN38.
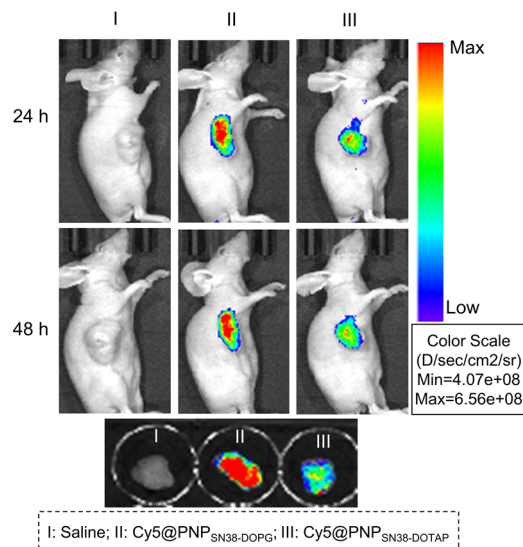

Fig. S16 The *in vivo* and *ex vivo* tumor accumulation profiles of Cy5-labeled PNP$_{SN38-DOTAP(1/2)}$ and PNP$_{SN38-DOPG(1/2)}$ at 24 or 48 h post injection.
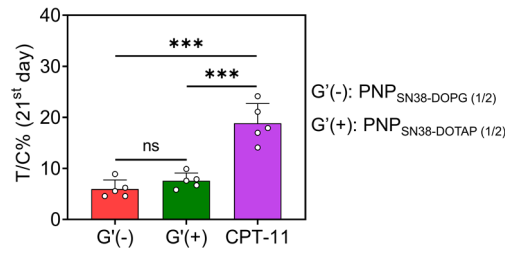
Fig. S17 Relative tumor growth rate (T/C%) of PNP$_{SN38-DOTAP(1/2)}$, PNP$_{SN38-DOPG(1/2)}$ and CPT-11 in xenograft HT-29 colorectal tumor models. All the formulations were injected *i.v.* at an equivalent dose of 15 mg/kg SN38 on every 3 days for 3 times.
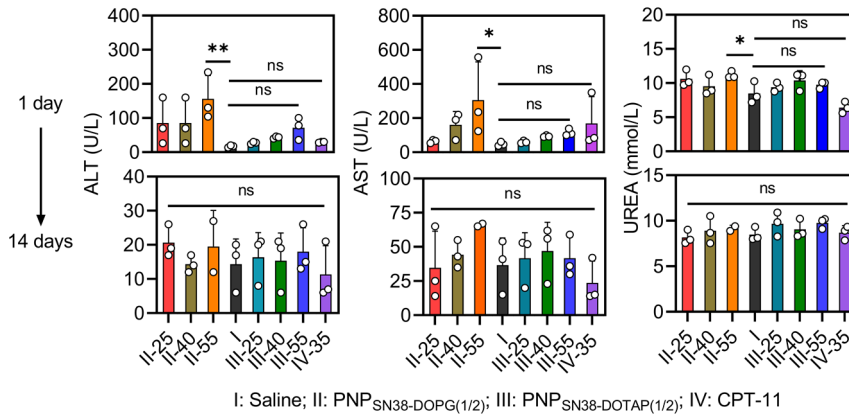

Fig. S18 Biochemical analysis of blood samples collected by retro-orbital bleeding into tubes without anticoagulant one or fourteen days after drug administration into KM mice. PNP$_{SN38-DOTAP(1/2)}$ and PNP$_{SN38-DOPG(1/2)}$ were intravenously injected at the dose of 25–55 mg/kg SN38, and CPT-11 was administered at equivalent dose of 35 mg/kg SN38. Statistical analysis was analyzed using one-way ANOVA with Tukey's multiple comparisons. Significance levels were defined as ns: no significant difference, $P > 0.05$, $*P < 0.05$, $**P < 0.01$.

Table S1. Particle size and size distributions of cationic, anionic and neutral lipid-assisted PEG-*b*-PLA nanoparticles prepared at various weight ratios.

Lipid	SN-38:lipid:PEG-*b*-PLA (w/w/w)	Average size (nm)	PDI	Zeta potential (mV)
DOTAP	1:0.1:10	124.9 ± 2.1	0.192 ± 0.003	21.4 ± 0.9
	1:0.2:10	121.7 ± 4.1	0.196 ± 0.010	21.4 ± 1.2
	1:0.5:10	115.8 ± 2.4	0.187 ± 0.005	21.5 ± 1.5
	1:1:10	114.9 ± 3.4	0.169 ± 0.012	31.4 ± 1.2
	1:2:10	109.4 ± 4.0	0.181 ± 0.014	32.4 ± 0.4
DOPG	1:0.1:10	113.0 ± 1.9	0.136 ± 0.008	-13.0 ± 0.6
	1:0.2:10	114.6 ± 1.9	0.162 ± 0.005	-15.2 ± 0.4
	1:0.5:10	106.0 ± 1.3	0.150 ± 0.009	-20.5 ± 0.6
	1:1:10	125.7 ± 1.6	0.196 ± 0.005	-31.8 ± 1.3
	1:2:10	117.0 ± 0.9	0.217 ± 0.010	-37.9 ± 0.7
HSPC	1:0.1:10	145.7 ± 4.1	0.385 ± 0.013	-1.1 ± 0.1
	1:0.2:10	127.6 ± 7.4	0.356 ± 0.043	-1.0 ± 0.1
	1:0.5:10	138.8 ± 3.8	0.188 ± 0.009	-1.7 ± 0.1
	1:1:10	127.5 ± 4.5	0.156 ± 0.006	-0.8 ± 0.3
	1:2:10	131.6 ± 4.3	0.179 ± 0.009	0.6 ± 0.2

Table S2. Physicochemical properties of cationic and anionic lipid-assisted PEG-*b*-PLA nanoparticles prepared at the weight ratio of SN38: Lipid: PEG-*b*-PLA = 1:0.5:10.

SN38-loaded formulations	Size (d.nm)	PDI	Zeta potentials (mV)	LE%
PNP$_{SN38-DOTAP (1/2)}$	115.8 ± 2.4	0.187 ± 0.005	21.5 ± 1.5	97.0 ± 4.5
PNP$_{SN38-DOPG (1/2)}$	106.0 ± 1.3	0.150 ± 0.009	-20.5 ± 0.6	93.2 ± 2.1